

Distinguishing Infiltrative Transitional Cell Carcinoma From Other Infiltrative Lesions of the Kidneys on Multidetector Computed Tomography

Pornphan Wibulpolprasert¹, Sasiwimon Jungtheerapanich¹, Bussanee Wibulpolprasert¹

¹ Department of Diagnostic and Therapeutic Radiology, Faculty of Medicine Ramathibodi Hospital, Mahidol University, Bangkok, Thailand

Background: The infiltrative renal growth pattern is either characteristic of certain prototype transitional cell carcinomas (TCCs) or other mimickers. Specific computed tomography (CT) features may be used to differentiate TCCs from other overlap findings. Accurate early diagnosis is important to improve treatment outcome and prevent morbidity and mortality from delayed specific treatment.

Objective: To determine the multidetector computed tomography (MDCT) features that discriminate infiltrative TCCs from other infiltrative renal lesions.

Methods: A retrospective review was performed on patients with infiltrative, proven renal lesions on CT from January 2008 to July 2014. Individual CT sequences were analyzed for lesion number, location, size, and density on unenhanced and nephrographic phase scans. Final diagnoses were confirmed by histopathology or clinical or imaging follow-up after treatment. The CT findings of intrarenal TCCs and mimics were compared by using logistic regression analysis.

Results: In 73 patients, there were 18 (24.6%) TCCs, 2 (2.7%) renal cell carcinomas (RCCs), 11 (15.1%) lymphomas, 15 (20.5%) renal parenchymal metastases, 17 (23.3%) infections, and 10 (13.7%) other diagnosis. Compared to non-TCCs, intrarenal TCCs were more likely to be solitary lesion, lack intralesional calcification, less avidly enhance in nephrographic phase and infiltrate pelvicalyceal and perinephric tissue ($P < .05$).

Conclusions: Five MDCT features including solitary lesion, absence of calcification and poor absolute, relative enhancement, pelvicalyceal system involvement, and perinephric tissue invasion were significantly associated with intrarenal and infiltrative TCCs.

Keywords: Infiltrative renal mass, Computed tomography, Transitional cell carcinoma

Rama Med J: doi:10.33165/rmj.2019.42.4.176646

Received: April 17, 2019 **Revised:** September 6, 2019 **Accepted:** December 2, 2019

Corresponding Author:

Pornphan Wibulpolprasert
Department of Diagnostic and Therapeutic Radiology,
Faculty of Medicine
Ramathibodi Hospital,
Mahidol University,
270 Rama IV Road, Ratchathewi,
Bangkok 10400, Thailand.
Telephone: +66 2201 1212
Fax: +66 2201 1297
E-mail: punlee77@gmail.com,
pornphan.wib@mahidol.ac.th





Introduction

Computed tomography (CT) has become the imaging procedure of choice in the investigation of virtually all abdominal complaints. As the number of abdominal imaging procedures has risen, and so too has the number of accidentally discovered renal lesions. Routine identification on cross-sectional imaging studies help to decrease the stage of the disease at presentation. A lesion involving the kidney can behave as a space-occupying mass with growth by expansion or permeates the renal parenchyma by interstitial infiltration. Of these 2 growth patterns, the most common primary renal tumors in adults (renal cell adenocarcinoma) and children (Wilms tumor) usually manifest as expansile masses. Infiltrative renal lesions are detected much less commonly than expansile, well-circumscribed solid renal lesions. Infiltrative lesions have ill-defined margins between normal renal parenchyma and the lesion but generally preserve the reniform contour with or without renal enlargement.¹ The infiltrative growth is either characteristic of certain renal tumors or tumor-like conditions.² In 1977, Ambos et al³ described the urographic and angiographic findings of infiltrative growth in 4 patients with lymphomas, metastases, transitional cell carcinomas (TCCs), and pleomorphic renal cell carcinomas (RCCs), respectively. However, the imaging findings on CT distinguishing TCCs from other infiltrative lesions have not been well described.

The purpose of this study was to determine which CT findings would be best discriminated TCCs from other mimics.

Methods

Study Design

The study was approved by the institutional review board and ethics committee on human subjects research (No. MURA2013/306 on May 21, 2013) with waiver of informed consent due to the retrospective review of all patients who underwent CT scan at Ramathibodi Hospital for suspected infiltrative renal lesions from January 2008 to July 2014.

Patient Selection

This retrospective cohort study included 73 patients aged 16 years or older with multidetector computed tomography (MDCT) who had a proven “infiltrative” or “ill-defined” renal lesion and were derived from a key word search of these terms in the institutional electronic radiology report record from the radiology information system. Final diagnosis was based on histopathology, or imaging or clinical follow-up and response to the specific treatment. Patients with incomplete information (ie, missing data, patient death or loss follow-up without final diagnosis) were excluded.

Data Collection

Patient Characteristic

Data elements collected from electronic medical records included patient age and gender, initial clinical presentation, history of underlying malignancy, recurrent urinary tract infection (UTI), pathological diagnosis, and/or clinical diagnosis with response to the specific treatment.

MCCT Imaging Technique

All CT scans of the kidney were performed at least non contrast and nephrographic phases by 1 of 3 different multidetector scanners: 1) 320 slices MDCT (Aquilion ONE; Toshiba Medical Systems Corp, Tokyo, Japan); 2) 128 slices MDCT (Aquilion CX; Toshiba Medical Systems Corp, Tokyo, Japan); 3) 64 slice MDCT (SOMATOM Sensation 64; Siemens Medical Solutions, Malvern, PA, USA).

All CT examinations were obtained during patient breath-holding with the following parameters for imaging acquisition and reconstruction: 120 kVp, automated tube current, a section thickness interval of 3 mm, section collimation 0.5×80 mm, rotation time 0.5 seconds, pitch factor 0.813, and helical pitch 65. Protocols varied depending on the type of examination. All patients received about 1000 mL of oral suspension (1000 mL of water and 20 mL contrast material) about 30 - 60 min before CT and 1.5 - 2 mL/kg (maximum 100 mL) of nonionic 300 - 320 mgI of intravenous (IV) contrast material; the IV contrast material was injected into antecubital vein

using a mechanical injector at a rate of 2.5 - 3.0 mL/sec, a bolus tracking algorithm was used to determine the onset of imaging of corticomedullary or arterial phase (30 - 40 seconds), nephrographic or venous phase (70 - 90 seconds). For bolus tracking, a region of interest (ROI) was placed in the thoracoabdominal aorta junction, with a trigger set to begin at 120 - 150 Hounsfield units (HU).

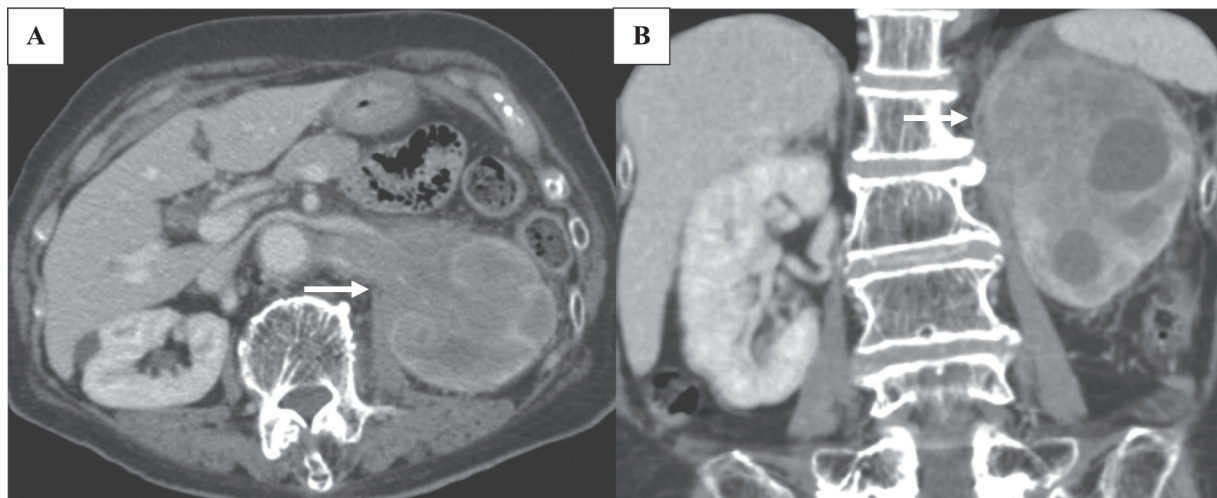
MDCT Findings and Analysis

All CT images of all cases were uploaded into a picture archiving and communications system (PACS) under DICOM conformance (Synapse Version 3.2.0, FUJIFILM Medical Systems USA's Synapse PACS System, USA).

All images were reviewed independently by an abdominal imaging attending radiologist and a last year diagnostic-radiology resident trainee blinded to clinical history. The readers confirmed each lesion as infiltrative based on preservation of renal contour and a poorly defined zone of transition between the lesion and normal renal parenchyma and/or renal collecting system^{1,2} (Figure 1). Lesion size was measured in the long axis single greatest dimension. If there are more than 1 lesion,

the largest lesion was measured. Lesion density on unenhanced scan was classified as hypo-, iso- or hyper-dense compared the surrounding renal parenchyma (30 - 40 HU) on non-enhanced CT scan. Hypo-dense lesions measured less than 30 HU and hyper-dense lesions measured between 41 HU to 90 HU.^{4,5} On nephrographic phase, renal mass enhancement was categorized as either homogenous or heterogeneous. Heterogeneous lesions had a combination of solid enhancing soft-tissue and non- or poorly- enhancing regions representing necrotic or cystic changes. Measurement of parenchymal enhancement in HU using 0.5 cm³ ROI placed within the enhancing regions of the mass but avoiding the necrotic regions and normal renal parenchyma. Larger ROI measurements were used in homogeneous solid masses and similarly placed on both the unenhanced and nephrographic phase scans.^{6,7} Degree of absolute nephrographic phase enhancement was categorized as mild (less than 97 HU), moderate (97 - 140 HU), and avid enhancement (greater than 140 HU). The cutoff points to separate tumors into mild, moderate, and avid enhancement groups were done, respectively.⁸

Figure 1. Computed Tomography (CT) Feature of Infiltrative Left Renal Lesion



A 58-year-old female presented with abdominal pain. Contrast-enhanced nephrographic phase axial (A) and coronal (B) multidetector computed tomography (MDCT) images showed infiltrative renal mass (transitional cell carcinoma [TCC]) at left upper pole (arrows) with preservation of reniform shape and associated with perinephric invasion. The mass caused focal obstruction, which seen as dilatation of calices.



Relative enhancement (RE) was calculated by measuring the change in density between the unenhanced and venous phase images using the following formula.

$$RE (\%) = \frac{\text{Contrast - Enhanced density} - \text{Unenhanced density}}{\text{Unenhanced density}} \times 100^9$$

The MDCT based pelvicalyceal system involvement was categorized into 5 patterns of tumor involvement as follows:⁹ 1) filling defect in pelvicalyceal system, which included pelvis and calyx; 2) focal mural thickening (focal thickening of any part of the collecting system); 3) diffuse mural thickening (diffuse thickening of any part of the collecting system); 4) focally obstruction, which is seen as dilatation of one or more calices with/without gross renal pelvis dilatation; and 5) lesion extending toward ureteropelvic junction tumor seen at ureteropelvic junction in connection with main tumor mass).

These additional described MDCT findings were also categorized: cystic and/or necrotic change, an area with low-attenuation (less than 20 HU on unenhanced scan without contrast enhancement);⁶ fat components (less than -10 HU);¹⁰ renal vein invasion by infiltrative lesion in the nephrographic phase with enhancing tumor thrombus; and invasion of perinephric tissue or renal sinus fat by the infiltrative lesion.¹¹

Statistical Analysis

Significant differences in MDCT findings between the TCCs subcohort and the other malignant and benign subcohorts were evaluated using chi-square test or Fisher exact test for categorical data and *t* test or Mann-Whitney test for continuous data. Mean, standard deviation (SD), median, and range were computed for all continuous data. Categorical data were summarized by using frequencies.

The association of specific imaging features between the TCCs subcohort and other infiltrative renal lesion subcohort was also evaluated by univariate and multivariate logistic regression analysis. The results were reported using odds ratio (OR), 95% confidence

interval (CI), and *P* value. For multivariate analysis, variables were selected from those that were significant in the univariate analysis.

The weighted kappa (K) score was used to measure interobserver agreement for the following findings: cystic or necrotic change, calcification, fat component, enhancement pattern, pelvicalyceal involvement, renal vein invasion, perinephric tissue or renal sinus fat invasion, intraabdominal lymphadenopathy, and other sites of malignancy. A K value of less than 0.20 was taken as poor agreement; 0.21 - 0.40, fair agreement; 0.41 - 0.60, moderate agreement; 0.61 - 0.80, good agreement; and 0.81 - 1.00, excellent agreement.¹² A *P* value of less than .05 was considered to be statistically significant finding. The STATA version 13 (Stata Corp. Version 13. College Station, TX: StataCorp LP; 2013) statistical software was used to analyze data.

Results

Patient Characteristics

Of 73 patients with infiltrative renal lesions in MDCT, there were TCCs subcohort [18 (24.6%)], infection subcohort [17 (23.3%)], renal metastasis subcohort [15 (20.5%)], and lymphoma subcohort [11 (15.1%)]. A variety of other lesions were also diagnosed: 4 cases (5.5%) of primary renal tumor with unknown histology, 2 cases (2.7%) of RCC as well as 1 case each (1.4%) of angiomyolipoma (AML), squamous cell carcinoma (SCC), immunoglobulin G4-related disease (IgG4-RD), and xanthogranulomatous pyelonephritis. There were 2 cases (2.7%) of inconclusive diagnosis between renal metastasis and infection.

In the 21 of 73 (28.8%) cases diagnosed by histopathology (11 cases of TCCs, 5 cases of infection, 2 cases of renal metastasis, and 1 case each of RCC, lymphoma and squamous cell carcinomas), specimens were obtained from partial (11.0%) and radical nephrectomy (8.2%), and percutaneous core needle biopsy (9.6%).



In 31 other cases, histopathology was from other sites, 18 cases (24.7%) from primary tumor (ie, bladder, bowel, lung, esophagus, larynx, and lymph node) and 13 cases (5.5%) from non-primary tumor (ie, liver, pelvic mass and lymph node). In 43 other cases (58.9%), the diagnosis was established using clinical and/or imaging follow-up after patients received specific treatment.

Interobserver agreement between 2 readers was tested for the following parameters: cystic or necrotic change, calcification, fat component, enhancement pattern, pelvicalyceal involvement, renal vein invasion, invasion of the perinephric tissue or renal sinus fat, intraabdominal lymphadenopathy, and other suspicious foci of malignancy. Excellent agreement was reported in all parameters ($K = 0.95 - 1.00$).

Comparison Between Intrarenal TCCs and Non-TCCs

The subcohort of patients with intrarenal TCCs were older (mean \pm SD, 68.9 ± 9.2 vs 56.4 ± 14.8 years;

$P = .001$), were more likely to present with gross hematuria ($P = .003$) (Table 1), and present unilaterally ($P = .003$) with a solitary lesion ($P = .001$), and had larger tumors (median [range], 7.7 [2.2 - 19.4] vs 5.5 [1.5 - 24.0] cm; $P = .05$), than patients in the non-TCC subcohorts. On the nephrographic phase scans, TCC subcohort enhanced significantly less than non-TCC subcohorts using both absolute (mean \pm SD, 69.2 ± 17.2 vs 83.0 ± 25.9 HU; $P = .04$), and relative enhancement (median [range], 100.2 [40.3 - 194.9] vs 150.1 [16.4 - 368.7] %; $P = .02$). Intrarenal TCCs invaded perinephric tissue significantly more frequently than non-TCCs (77.8% vs 41.8%; $P = .01$). Both invasion of renal vein (27.8% vs 14.6%), and the presence of intraabdominal lymphadenopathy, and other suspicious foci of malignancy were more common in intrarenal TCCs than non-TCCs but this difference was not significant. Presence of pelvicalyceal involvement was significantly more common in intrarenal TCCs, compared to non-TCCs ($P < .001$) (Table 2).

Table 1. Baseline Characteristic of Patients With Infiltrative Renal Lesions Stratified by Diagnosed of Intrarenal TCCs and Non-TCCs (N = 73)

Parameter	No. (%)			<i>P</i> Value*
	Total (N = 73)	TCCs (n = 18)	Non-TCCs (n = 55)	
Age, mean \pm SD, y	59.5 \pm 14.6	68.9 \pm 9.2	56.4 \pm 14.8	.001
Gender				
Male	26 (35.6)	6 (33.3)	20 (36.4)	
Female	47 (64.4)	12 (66.7)	35 (63.6)	.82
Presenting symptoms				
Gross hematuria	12 (16.4)	7 (38.9)	5 (9.1)	.003
Abdominal/flank pain	18 (24.7)	4 (22.2)	14 (25.5)	1.00
Underlying malignancy	27 (37.0)	4 (22.2)	23 (41.8)	1.00

Abbreviations: SD, standard deviation; TCC, transitional cell carcinoma.

* $P < .05$ was considered statistically significant.



Table 2. Imaging Features of Intrarenal TCCs and Non-TCCs in Infiltrative Renal Lesions (N = 73)

Feature	No. (%)		P Value*	OR (95% CI)**
	TCCs (n = 18)	Non-TCCs (n = 55)		
Side of tumor				
Unilateral	18 (100.0)	35 (63.6)	.003	-
Bilateral	0 (0)	20 (36.4)		
Size of tumor, median (range), cm	7.7 (2.2 - 19.4)	5.5 (1.5 - 24.0)	.05	-
Number of tumor				
Solitary	17 (94.4)	29 (52.7)	.001	15.20 (1.90 - 122.60)
Multiple	1 (5.6)	26 (46.3)		
Density, HU				
Pre-contrast	35.0 ± 5.1	32.4 ± 7.2	.16	-
Post-contrast	69.2 ± 17.2	83.0 ± 25.9	.04	-
Enhancement RE, median (range), %	100.2 (40.3 - 194.9)	150.1 (16.4 - 368.7)	.02	0.99 (0.98 - 0.99)
Enhancement pattern				
Homogeneous	1 (5.6)	6 (10.9)	.67	-
Heterogeneous	17 (94.4)	49 (89.1)		
Pelvicalyceal involvement	18 (100.0)	17 (30.9)	< .001	-
Renal vein invasion	5 (27.8)	8 (14.6)	.41	-
Invasion of perinephric tissue	14 (77.8)	23 (41.8)	.01	4.90 (1.40 - 16.70)
Intraabdominal lymphadenopathy	9 (50.0)	26 (47.3)	.84	-
Suspicious foci of malignancy	9 (50.0)	37 (67.3)	.19	-

Abbreviations: CI, confidence interval; OR, odds ratio; RE, relative enhancement; TCC, transitional cell carcinoma.

* $P < .05$ was considered statistically significant.

** OR was determined by using univariate regression analysis.

However, when pelvicalyceal system involvement was subdivided into filling defects in pelvicalyceal system, focal or diffuse mural thickening, focally obstruction and extension to ureteropelvic junction between intrarenal TCCs and others infiltrative renal lesion, there was no difference in each CT finding (Figure 2).

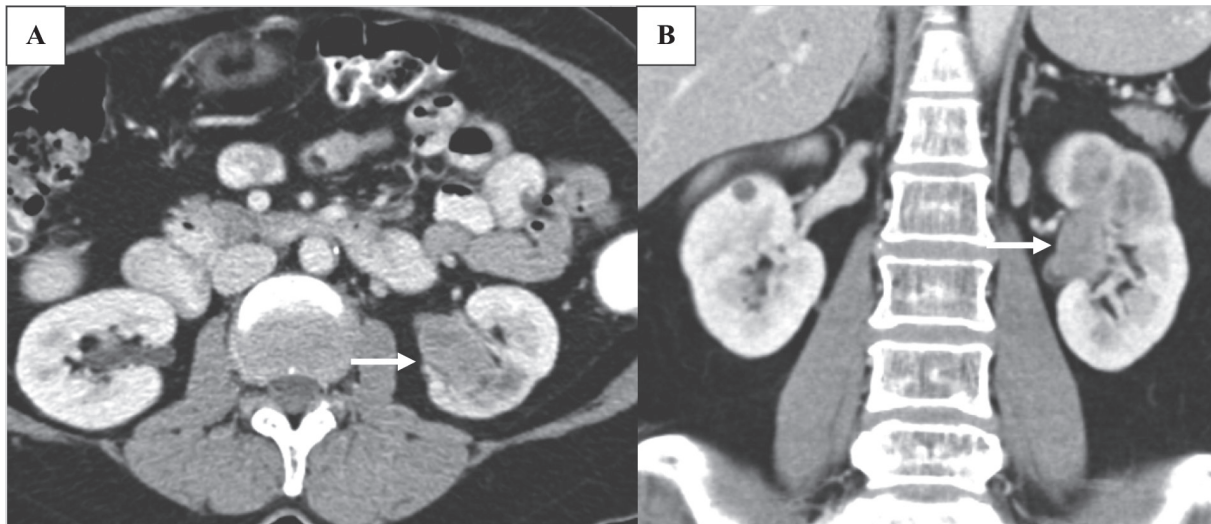
In multivariate logistic regression analysis, the 2 features of solitary lesion and less relative enhancement were significantly associated with intrarenal TCCs (OR, 13.28, $P = .02$; and OR, 0.99, $P = .04$, respectively) compared to non-TCCs. The contrast-enhanced MDCTs

between infiltrative intrarenal TCCs and non-TCCs (focal pyelonephritis) were measured (Figure 3).

Comparison Between Intrarenal Lymphoma and Non-Lymphoma

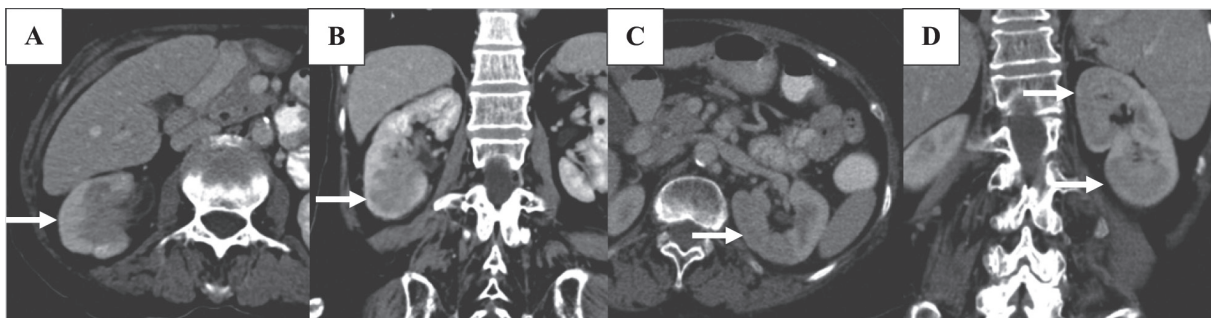
The 11 patients (15.1%) in the intrarenal lymphoma subcohort were significantly more likely to have multiple lesions with bilateral renal involvement ($P = .02$ and $P = .001$, respectively) and have homogeneous enhancement patterns (4 lymphoma patients [36.4%] and 3 non-lymphoma patients [4.8%], $P = .008$).

Figure 2. Presence of Pelvicalyceal Involvement in Intrarenal Transitional Cell Carcinoma (TCC)



Contrast-enhanced nephrographic phase axial (A) and coronal (B) multidetector computed tomography (MDCT) of a 69-year-old female with hematuria showed infiltrative enhancing lesion (transitional cell carcinoma) in the left kidney with pelvicalyceal system involvement (arrow).

Figure 3. Comparison of Contrast-Enhanced Multidetector Computed Tomography (MDCT) Between Intrarenal Transitional Cell Carcinoma (TCC) and Focal Pyelonephritis



Contrast-enhanced nephrographic phase axial (A) and coronal (B) images of pathologically proved intrarenal TCC showed infiltrative heterogeneous enhancing renal mass at right lower pole (arrow). The relative enhancement is measured approximately 146.7%. Another patient with pyelonephritis, contrast-enhanced nephrographic phase axial (C) and coronal (D) showed infiltrative lesion at left upper and lower poles (arrows). The relative enhancement is measured approximately 353.3%.

Comparison Between Renal Metastasis and Non-Metastasis

Of the 15 patients (20.6%) in the renal metastasis subcohort, the most common sources of primary malignancies were lung (35.7%), esophagus (21.4%), adenocarcinoma

(14.3%), cholangiocarcinoma (7.1%), colon cancer (7.1%), laryngeal cancer (7.1%), and melanoma (7.1%). No specific radiographic characteristics distinguish between renal metastasis and other infiltrative renal lesions.



Comparison Between Lesions Related to Renal Infection and Non-Infection

Of the 17 patients (23.3%) in the infection subcohort, 5 cases were pathologically proven with nephrectomy and US-guided kidney biopsy, 4 patients of pyelonephritis, and 1 patient of renal abscess, respectively. A combination of clinical findings, imaging findings, positive urinalysis, and cultures were used to diagnose pyelonephritis in the other 12 patients.

The common imaging features favoring a lesion related to intrarenal infection were an absence of cystic or necrotic change, pelvicalyceal system involvement, renal vein, and perinephric tissue invasion and intraabdominal lymphadenopathy. After contrast injection, the infected lesion subcohort had density, and relative enhancement greater than the non-infection subcohorts (214.9% [range, 92.5 - 353.3] vs 114.2% [range, 16.4 - 368.]; $P < .01$).

Discussion

A contrast-enhanced CT is the standard imaging test for initial detection of an infiltrative renal mass. This study showed that a combination of features including the concept of relative enhancement, characterization of these lesions is possible at initial diagnosis potentially avoiding more invasive, uncomfortable and morbid procedures for patients such as renal biopsy. In most cases, CT diagnosis especially in the context of clinical and laboratory information (eg, symptoms of UTI with positive urinalysis or culture) is straightforward and treatment can be confidently planned. However, in a significant minority of renal lesions, a single confident diagnosis is not possible since additional information is unhelpful and differential diagnosis for these lesions includes TCC, RCC, renal lymphoma, renal metastasis, and infection of the kidney, prompting either short interval follow-up or biopsy.

Several previous reports^{9, 13, 14} have described the imaging characteristics of intrarenal TCC, which should be suspected in the presence of an infiltrating renal mass with pelvic filling defects or if any part of the

collecting system is irregular, narrowed, or amputated. Pickhardt et al¹ described intrarenal TCC arising from the renal pelvic urothelium with infiltration in and around the pelvicalyceal system.

Raza et al⁹ described the most diagnostic signs of intrarenal TCC which were a filling defect in the renal pelvis, tumor center perceived in the renal pelvis, renal shape preservation, the absence of cystic or necrotic change, homogeneity of the tumor and extension in to the ureteropelvic junction. Hartman et al¹³ also reported that invasive TCC is suspected when an infiltrative renal mass coexists with a pelvic filling defect or irregular narrowing or amputation of the collecting system.

In the present study, the findings that favored intrarenal TCC were single, unilateral lesions, absence of calcification, less absolute and relative lesion enhancement, and invasion of either pelvicalyceal system and/or perinephric tissue.

Relative enhancement has been shown to be of value in the CT discrimination of clear cell renal cell carcinoma from other cortical lesions. Less absolute and relative enhancement of the intrarenal TCC relative to other infiltrative renal lesions is similar to studies by Phatak et al¹⁵ and Leder et al¹⁶ who reported that TCC typically had minimal enhancement after intravenous contrast compared to much more hypervascular renal cell carcinoma.

Yousem et al¹⁷ reported synchronous TCC was found in 2.3% of patients with bladder TCC, 39% of those with ureteral TCC, and 24% of those with renal TCC. Metachronous upper-tract tumors developed in 13% of patients with primary ureteral TCC and in 11% of with renal TCC, after average delays of 28 and 22 months, respectively. In the present study, although most of intrarenal TCC were single and unilateral, there was a case with a synchronous lesion in urinary bladder. In another intrarenal TCC case, a metachronous lesion developed in the urinary bladder 2 years after diagnosis.

Several studies have shown that the most commonly encountered pattern of involvement in patients with renal lymphoma was multiple bilateral masses within the renal cortex due to its hematogenous nature.¹⁸⁻²¹



Diffuse infiltration is almost always bilateral and is seen in approximately 20% of patients. In this study, renal lymphoma was most commonly presented with multifocal and bilateral involvement with homogeneous enhancement, unlike the usually heterogeneous enhancement in renal cell carcinoma.²¹

Prkacin et al²² reported that carcinoma of the lung was the most common origin of renal metastases as was confirmed in this study, where 35.7% of metastatic lesion were of lung origin. Although they reported that metastases tended to be small, multiple, less exophytic, with or without wedge shaped appearance compared to renal cell carcinoma. This study found that no specific imaging feature to distinguish renal metastasis from other infiltrative renal lesions. Diagnosis was determined mainly from history of known malignancy.

Finally, this study showed that renal infection related infiltrative lacked cystic or necrotic change and intraabdominal lymphadenopathy, and also lacked involvement of the pelvicalyceal system, renal vein and perinephric tissue. In addition, the same findings were found in benign lesion as well.

There are some limitations in this study. The small sample size is the most important limitation in this study because infiltrative renal lesion is relatively rare as compared

with well-defined solid cortical renal lesions. Second, the retrospective nature resulted in some missing data in the clinical information. Third, most of the lesions had no pathological confirmation. Finally, there were certain numbers of lesion diagnosed by correlation with clinical and laboratory findings or follow-up images rather than histopathology. A much larger prospective trial would be of value to independently test the findings of this study and to determine their true clinical utility.

Conclusions

This study showed that 5 MDCT features help to discriminate intrarenal TCC from other infiltrative lesions: solitary lesion, pelvicalyceal system involvement, perinephric tissue invasion, absence of calcification and poor absolute, and relative enhancement.

Acknowledgements

The authors acknowledge Professor Dr. Steven S Raman, diagnostic and interventional radiologist at UCLA, California, for review and editing of the draft manuscript; and Professor Dr. Amnuay Thithapandha, Mahidol University, Thailand, for review and editing of the revised manuscript.

References

1. Pickhardt PJ, Lonergan GJ, Davis CJ Jr, Kashitani N, Wagner BJ. From the archives of the AFIP. Infiltrative renal lesions: radiologic-pathologic correlation. Armed Forces Institute of Pathology. *Radiographics*. 2000;20(1):215-243. doi:10.1148/radiographics.20.1.g00ja08215.
2. Hecht EM, Hindman N, Huang WC, Rosenkrantz AB, Melamed J. Extensive infiltrating renal cell carcinoma with minimal distortion of the renal anatomy mimicking benign renal vein thrombosis. *Am J Kidney Dis*. 2010;55(5):967-971. doi:10.1053/j.ajkd.2009.09.030.
3. Ambos MA, Bosniak MA, Madayag MA, Lefleur RS. Infiltrating neoplasms of the kidney. *AJR Am J Roentgenol*. 1977;129(5):859-864. doi:10.2214/ajr.129.5.859.
4. Silverman SG, Mortele KJ, Tuncali K, Jinzaki M, Cibas ES. Hyperattenuating renal masses: etiologies, pathogenesis, and imaging evaluation. *Radiographics*. 2007;27(4):1131-1143. doi:10.1148/rg.274065147.
5. Bosniak MA. The small (less than or equal to 3.0 cm) renal parenchymal tumor: detection, diagnosis, and controversies. *Radiology*. 1991;179(2):307-317. doi:10.1148/radiology.179.2.2014269.
6. Israel GM, Bosniak MA. How I do it: evaluating renal masses.

Radiology. 2005;236(2):441-450. doi:10.1148/radiol.2362040218.

7. Kim JK, Kim TK, Ahn HJ, Kim CS, Kim KR, Cho KS. Differentiation of subtypes of renal cell carcinoma on helical CT scans. *AJR Am J Roentgenol.* 2002;178(6):1499-1506. doi:10.2214/ajr.178.6.1781499.

8. Zhang J, Lefkowitz RA, Ishill NM, et al. Solid renal cortical tumors: differentiation with CT. *Radiology.* 2007;244(2):494-504. doi:10.1148/radiol.2442060927.

9. Raza SA, Sohaib SA, Sahdev A, et al. Centrally infiltrating renal masses on CT: differentiating intrarenal transitional cell carcinoma from centrally located renal cell carcinoma. *AJR Am J Roentgenol.* 2012;198(4):846-853. doi:10.2214/AJR.11.7376.

10. Davenport MS, Neville AM, Ellis JH, Cohan RH, Chaudhry HS, Leder RA. Diagnosis of renal angiomyolipoma with Hounsfield unit thresholds: effect of size of region of interest and nephrographic phase imaging. *Radiology.* 2011;260(1):158-165. doi:10.1148/radiol.11102476.

11. Prando A, Prando P, Prando D. Urothelial cancer of the renal pelvicaliceal system: unusual imaging manifestations. *Radiographics.* 2010;30(6):1553-1566. doi:10.1148/rg.306105501.

12. McHugh ML. Interrater reliability: the kappa statistic. *Biochem Med (Zagreb).* 2012;22(3):276-282.

13. Hartman DS, Davidson AJ, Davis Jr CJ, Goldman SM. Infiltrative renal lesions: CT-sonographic-pathologic correlation. *AJR Am J Roentgenol.* 1988;150(5):1061-1064. doi:10.2214/ajr.150.5.1061.

14. Bree RL, Schultz SR, Hayes R. Large infiltrating renal transitional cell carcinomas: CT and ultrasound features. *J Comput Assist Tomogr.* 1990;14(3):381-385.

15. Phatak SV, Kolwadkar PK. Renal and ureteral transitional cell carcinoma: a case report. *Indian J Radiol Imaging.* 2006;16(4):907-909. doi:10.4103/0971-3026.32381.

16. Leder RA, Dunnick NR. Transitional cell carcinoma of the pelvicalices and ureter. *AJR Am J Roentgenol.* 1990;155(4):713-722. doi:10.2214/ajr.155.4.2119098.

17. Yousem DM, Gatewood OM, Goldman SM, Marshall FF. Synchronous and metachronous transitional cell carcinoma of the urinary tract: prevalence, incidence, and radiographic detection. *Radiology.* 1988;167(3):613-618. doi:10.1148/radiology.167.3.3363119.

18. Cohan RH, Dunnick NR, Leder RA, Baker ME. Computed tomography of renal lymphoma. *J Comput Assist Tomogr.* 1990;14(6):933-938.

19. Richmond J, Sherman RS, Diamond HD, Craver LF. Renal lesions associated with malignant lymphomas. *Am J Med.* 1962;32:184-207. doi:10.1016/0002-9343(62)90289-9.

20. Heiken JP, Gold RP, Schnur MJ, King DL, Bashist B, Glazer HS. Computed tomography of renal lymphoma with ultrasound correlation. *J Comput Assist Tomogr.* 1983;7(2):245-250.

21. Urban BA, Fishman EK. Renal lymphoma: CT patterns with emphasis on helical CT. *Radiographics.* 2000;20(1):197-212. doi:10.1148/radiographics.20.1.g00ja09197.

22. Prkaćin I, Naumovski-Mihalić S, Dabo N, Palcić I, Vujanić S, Babić Z. Comparison of CT analyses of primary renal cell carcinoma and of metastatic neoplasms of the kidney. *Radiol Oncol.* 2001;35(2):105-110.

การแยกมะเร็งของไทดันดิเซลล์ทรายซิชันนอลออกจากพยาธิสภาพอื่นที่มีลักษณะ ขอบเขตไม่ชัดเจนจากภาพเอกซเรย์คอมพิวเตอร์

พรพรรณ วิบูลผลประเสริฐ¹, ศศิวิมล จึงธีรพานิช¹, บุญฤทธิ์ วิบูลผลประเสริฐ¹

¹ ภาควิชารังสีวิทยา คณะแพทยศาสตร์โรงพยาบาลรามาธิบดี มหาวิทยาลัยมหิดล กรุงเทพฯ ประเทศไทย

บทนำ: ลักษณะของก้อนในไทดที่ขอบเขตไม่ชัดเจนเป็นลักษณะจำเพาะอย่างหนึ่งของมะเร็งไทดันดิเซลล์ทรายซิชันนอล (Transitional cell carcinoma, TCC) และอาจเกิดจากสาเหตุอื่นได้ เช่น ก้อน การวินิจฉัยที่ลูกด้วยและรวดเร็ว มีความสำคัญอย่างยิ่งที่จะช่วยให้ผู้ป่วยได้รับผลการรักษาที่ดีที่สุด

วัสดุประสงค์: เพื่อระบุลักษณะจากภาพเอกซเรย์คอมพิวเตอร์ (Multidetector computed tomography, MDCT) ในการแยกมะเร็งของไทดันดิเซลล์ทรายซิชันนอลออกจากพยาธิสภาพอื่น

วิธีการศึกษา: การศึกษาข้อมูลในกลุ่มผู้ป่วยที่มีลักษณะก้อนในไทดที่ขอบเขตไม่ชัดเจนจากภาพเอกซเรย์คอมพิวเตอร์ ในช่วงเดือนกรกฎาคม พ.ศ. 2551 ถึงเดือนกรกฎาคม พ.ศ. 2557 ลักษณะต่างๆ ที่เห็นจากภาพเอกซเรย์คอมพิวเตอร์ นำมาเปรียบเทียบกับผลการวินิจฉัยสุดท้ายโดยผลพิสูจน์ขึ้นเนื่องหรือการติดตามอาการและติดตามภาพถ่ายรังสี จากนั้นทำการวิเคราะห์โดยใช้สหัศพติ Logistic regression analysis

ผลการศึกษา: ผู้ป่วยจำนวน 73 คน ที่มีก้อนขอบเขตไม่ชัดเจนในไทด แบ่งเป็น มะเร็งไทดันดิเซลล์ทรายซิชันนอล จำนวน 18 คน คิดเป็นร้อยละ 24.6 มะเร็งไทดันดิเซลล์เนื้อเยื่อไทด (Renal cell carcinoma, RCC) จำนวน 2 คน คิดเป็นร้อยละ 2.7 มะเร็งไทดจากเซลล์มะเร็งต่อมน้ำเหลือง (Lymphoma) จำนวน 11 คน คิดเป็นร้อยละ 15.1 มะเร็งไทดจากการกระจายมะเร็งของอวัยวะอื่น (Renal parenchymal metastasis) จำนวน 15 คน คิดเป็นร้อยละ 20.5 ก้อนเนื้อในไทดจากการติดเชื้อ จำนวน 17 คน คิดเป็นร้อยละ 23.3 และก้อนเนื้อในไทดจากสาเหตุอื่นๆ จำนวน 10 คน คิดเป็นร้อยละ 13.7 โดยมะเร็งไทดันดิเซลล์ทรายซิชันนอลมีแนวโน้มที่จะมีลักษณะเป็นก้อนเดี่ยว ไม่มีหินปูนภายในก้อน ก้อนมีสัญญาณความเข้มหลังนีดสารทึบสีน้ำเงินสีน้ำเงินตื้น ลักษณะรูปคล้ายไข่ต้ม แต่ไม่ลักษณะรูปคล้ายไข่ต้มที่พบในมะเร็งไทดันดิเซลล์ทรายซิชันนอล แต่ลักษณะรูปคล้ายไข่ต้มที่พบในมะเร็งไทดันดิเซลล์ทรายซิชันนอล มีลักษณะรูปไข่ต้มที่มีหินปูนภายในก้อน ไม่มีสัญญาณความเข้มหลังนีดสารทึบสีน้ำเงินสีน้ำเงินตื้น ลักษณะรูปคล้ายไข่ต้ม แต่ไม่ลักษณะรูปคล้ายไข่ต้มที่พบในมะเร็งไทดันดิเซลล์ทรายซิชันนอล

สรุป: ลักษณะสำคัญ 5 ประการ จากภาพเอกซเรย์คอมพิวเตอร์ของก้อนเนื้อในไทดที่มีขอบเขตไม่ชัดเจน ได้แก่ การเป็นก้อนเดี่ยว ไม่มีหินปูนภายในก้อน สัญญาณความเข้มหลังนีดสารทึบสีน้ำเงินสีน้ำเงินตื้น ลักษณะรูปคล้ายไข่ต้มที่พบในมะเร็งไทดันดิเซลล์ทรายซิชันนอล แต่ไม่ลักษณะรูปคล้ายไข่ต้มที่พบในมะเร็งไทดันดิเซลล์ทรายซิชันนอล และเนื้อเยื่อรอบไวด เป็นลักษณะที่ลับพันธุ์กับมะเร็งของไทดันดิเซลล์ทรายซิชันนอล เมื่อเปรียบเทียบกับพยาธิสภาพอื่นอย่างมีนัยสำคัญ ($P < .05$)

คำสำคัญ: ก้อนในไทดที่ขอบเขตไม่ชัดเจน เอกซเรย์คอมพิวเตอร์ มะเร็งไทดันดิเซลล์ทรายซิชันนอล

Rama Med J: doi:10.33165/rmj.2019.42.4.176646

Received: April 17, 2019 Revised: September 6, 2019 Accepted: December 2, 2019

Corresponding Author:

พรพรรณ วิบูลผลประเสริฐ
ภาควิชารังสีวิทยา คณะแพทยศาสตร์
โรงพยาบาลรามาธิบดี
มหาวิทยาลัยมหิดล กรุงเทพฯ ประเทศไทย
270 ถนนพระรามที่ 6
แขวงทุ่งพญาไท เขตราชเทวี
กรุงเทพฯ 10400 ประเทศไทย
โทรศัพท์ +66 2201 1212
โทรสาร +66 2201 1297
อีเมล punlee77@gmail.com,
pormphan.wib@mahidol.ac.th

